Indian Journal of Radio & Space Physics
Vol 43, February 2014, pp 67-74

A case study of gravity waves observed in OH rotational temperatures at Kolhapur (16.8ºN, 74.1ºE), India

Navin Parihar[1,$,*] & G K Mukherjee[2,#]

[1]Dr KSKGR Lab, Indian Institute of Geomagnetism, Allahabad 221 505, India

[2]C-309, Bhanushanti No 2 CHS Ltd, Rani Sati Marg, Malad (E), Mumbai 400 097, India

E-mail: [$]navindeparihar@gmail.com; [#]gkmiig@yahoo.co.in

Received 16 May 2013; revised 14 August 2013; accepted 16 September 2013

Ground-based measurements of OH (8, 3) Meinel band emissions were carried out at Kolhapur (16.8ºN, 74.1ºE), India during November 2002 – May 2003 using two tilting filter photometers. OH rotational temperature ~ a proxy of atmospheric temperature around 87 km, were derived from the intensity information of $P_1(2)$ and $P_1(4)$ lines of OH (8, 3) band. On most nights, strong well-defined oscillations having periodicities in the range of 1 – 3 h were observed in OH temperature series. In this paper, a case study of such short-period oscillations, observed on few nights in the OH temperature, has been presented.

Keywords: Gravity wave, Short period oscillation, Airglow emission, Nightglow emission

PACS Nos: *92.60.hh*; *92.60.hw*

1 Introduction

Gravity waves (GWs) are the important dynamical drivers of the mesosphere-lower thermosphere (MLT) region. GWs are the atmospheric oscillations created by the action of gravity on the density variations in the stratified troposphere from the passage of wind over topographic structures, wind shears, convective activity, lightning and thunderstorms, etc. (Ref. 1 and references therein). They have periods ranging from few minutes to few hours, and have horizontal wavelengths of few kilometres to few thousand kilometres. These waves propagate upwards as well as horizontally with amplitude growing with height (due to decreasing density). At MLT altitudes, they become convectively unstable attaining the saturation limit and ultimately break, thereby, dissipating momentum and energy to the background atmosphere. Briefly, GWs significantly influence the mean state of the mesopause region through energy and momentum deposition, diffusion and vertical transport of chemical species, etc.[2,3] Globally, GWs are highly variable in nature with reference to occurrence and propagation characteristics[4]. The propagation of GWs is greatly influenced by the background winds. Depending upon the direction of wind, the Doppler shifting of the wave parameters or loss of the wave energy to mean flow or reflection or the directional filtering effect may take place. As such, the gravity wave parameters, inferred using the ground-based measurements of airglow emissions, represent the apparent Doppler shifted characteristics of GWs and their intrinsic properties can be determined in the light of the proper wind information[5,6].

With reference to airglow process, GWs on course of their propagation in the MLT region affect the density of chemical species within the emission layer and its ambient temperature, which in turn affects the rate of reaction producing airglow. As such, GWs are observed as the wave-like features in airglow intensity and in temperature derived from airglow. Following this, ground-based measurements of nightglow features emanating from the MLT region have been widely used to study gravity wave phenomenology. For example, Fagundes *et al.*[7] investigated gravity wave phenomenology using ground-based measurements OI 557.7 nm, O_2 (0, 1) atmospheric band, NaD and OH (9, 4) Meinel band nightglow, and found that short-period quasi-coherent temporal variations superimposed on the large temporal intensity variations. Most recently, Bageston *et al.*[8] and Li *et al.*[9] investigated gravity waves in OH airglow images and found the periods laying between 5 and 20 min. At Norwegian Andøya Rocket Range (ARR, 69.3°N) and Swedish Rocket Range

(Esrange, 67.9°N), MaCWAVE (Mountain and Convective Waves Ascending VErtically) programme was conducted during 2002-2003 to address gravity wave processes in the MLT region using ALOMAR MF and MST radars and RMR and Na lidars, Esrange MST and meteor radars and RMR lidar, radiosondes, all-sky imager and TIMED (Thermosphere Ionosphere Mesosphere Energetics and Dynamics) satellite measurements of thermal structures[10,11]. In Indian subcontinent, Mukherjee[12] investigated the propagation characteristics of small-scale gravity waves using OH and OI 557.7 nm imaging observations at Panhala (17.0ºN, 74.2ºE); Dutta *et al.*[13] reported seasonal variation of short-period (< 2 h) gravity waves over Gadanki (13.5ºN, 79.2ºE) using VHF radar wind data. Mukherjee *et al.*[14] inferred the horizontal propagation characteristics of gravity waves using OH and OI 557.7 imaging observations and investigated the effect of filtering of gravity waves by the neutral wind flow. Lakshmi Narayanan & Gurubaran[15] studied the characteristics of high frequency gravity waves over Tirunelveli (8.7ºN, 77.8ºE) using OH imaging data. Taori *et al.*[16] investigated the dominant wave harmonics in 40-95 km altitude range and their propagation characteristics using OH and O_2 temperatures along with the lidar measurements over Gadanki (13.5ºN, 79.2ºE), India. In present study, ground-based nightglow observations of $P_1(2)$ and $P_1(4)$ line emissions of OH (8, 3) Meinel band were carried out at Kolhapur (16.8ºN, 74.1ºE), India during November 2002 – May 2003 using two tilting filter photometers. The OH rotational temperatures ~ a proxy of atmospheric temperature around OH emission peak of 87 km, were inferred from the knowledge of intensity of $P_1(2)$ and $P_1(4)$ rotational lines. A statistical account of these OH rotational temperature measurements has been presented earlier by Mukherjee & Parihar[17]. The chief objective of these temperature measurements was to examine gravity wave activity in the temperature field of the upper mesospheric region around OH emission peak of 87 km. The nocturnal behaviour of OH temperature on most occasions was marked by wave-like features. In this paper, an account of short-period waves observed in OH (8, 3) temperature on few nights during November 2002 – May 2003 has been presented.

2 Experimental set up and Data processing

Nightglow measurements of $P_1(2)$ – 731.64 nm and $P_1(4)$ – 736.95 nm line of OH (8, 3) Meinel band were carried out at Kolhapur (16.8ºN, 74.1ºE), India during November 2002 – May 2003 using two tilting filter photometers. The details of these tilting filter photometers for nightglow observations have been presented by Mukherjee & Dyson[18]. The two photometers were fixed for observations along zenith only and each had a field of view of 1°. Each photometer utilized a Thorn EMI 9658B photomultiplier tube thermoelectrically cooled at – 25ºC for photon detection. In the normal position of optical filter, the photometer provides the intensity information of both the nightglow feature and the background emission; whereas it gives the intensity of background emissions in the tilted mode of filter. And the difference of two measurements can be used to infer the intensity of the nightglow feature. Using the information of the transparency of filters, photomultiplier dark current and sensitivity of the photomultiplier tube with respect to a particular wavelength, the necessary corrections were incorporated in the intensity data. Due to non-availability of a standard source of light, the absolute calibration of the intensity in Rayleigh could not be performed.

It is well known that the intensity of the P - lines of OH Meinel band depends on the rotational temperature of OH molecule as given by following expression[19]:

$$I(J'',\upsilon'' \leftarrow J',\upsilon') = N_{\upsilon'}\bar{A}(J'',\upsilon'' \leftarrow J',\upsilon')\frac{2(2J'+1)}{Q_{\upsilon'}(T_{rot})}e^{-\frac{E_{\upsilon'}(J')}{kT_{rot}}} \quad \ldots (1)$$

where J', J'', are rotational quantum numbers (single primed quantities represent upper state and double primed ones the lower state); υ', υ'', vibrational quantum numbers; $N_{\upsilon'}$, the total concentration of the molecules in upper vibrational state; $\bar{A}(J'', \upsilon'' \leftarrow J', \upsilon')$, Einstein transition probability for indicated transition; $E_{\upsilon'}(J')$, the upper state term value; k, Boltzmann constant; T_{rot}, the rotational temperature; and $Q_{\upsilon'}(T_{rot})$, the partition function of the upper vibrational state. Knowing $\bar{A}$, J' and $E_{\upsilon'}(J')$, the ratio of intensity of two emission lines of a Meinel band can be used to infer OH rotational temperature. Assuming that the excited OH molecule is well thermalized prior to emission, this OH rotation temperature can be taken as a proxy of atmospheric temperature of ~87 km altitude. Herein, OH (8, 3) rotational temperatures were derived from the ratio of intensity of $P_1(2)$ and $P_1(4)$ line (an elaborative

account of the temperature retrieval from intensity measurements has been presented earlier[20]). The term values given by Kendall & Clark[21] and transition probabilities estimated by Langhoff *et al.*[22] have been used here.

The estimated uncertainty in the derived temperatures was ~5 K. The time resolution of temperature data was 5 minutes. Over 100 number of temperature measurements (encompassing 8 hours of observations) existed in each temperature series, in general, and this ensured good investigation of short-period wave features. On the whole, around 60 nights of observations was available during November 2002 – May 2003. However, the wave features were observed on only 60% of the nights. Here, the investigations of short-period oscillations on few nights marked by strong gravity wave activity are presented. The number of nights with very short data coverage of ~4 hours was very less, and generally, the duration of continuous observation was more than 6–7 hours. As the intensity were not calibrated and the wave features were more pronounced in temperature series (when compared with the intensity observations), the temperature database was taken into consideration to study the gravity wave induced perturbations. In this context, it is worthy to mention here that the intensity and temperature variations on most of the nights were highly correlated (the coefficient of correlation being ~0.90 on most occasions)[20]. The horizontal propagation characteristics (viz phase speed and wavelength) of observed gravity waves could not be inferred as the photometers looked along zenith only. Furthermore, the vertical propagation of these waves could not be investigated due to the lack of measurement of other nightglow features originating from higher altitudes.

3 Observations and Analysis

Figure 1 presents some typical examples of gravity wave induced variations in the nocturnal behaviour of OH temperature (the temporal evolution is presented in IST hours). Also shown in the individual plots are the 3-points running average (represented by the solid curves) and have been applied for smoothing the observed variations. In all the plots, the prominent short period (~1–2 h) wave-like oscillatory features can clearly be seen. On most of the nights shown in Fig. 1, gravity wave induced oscillations (GWOs) were found to be superimposed over a long period tide-like feature. On 04-05 November 2002, GWOs appear to be riding over a ter-diurnal tidal feature. The oscillatory features can be seen over a diurnal trend on 04-05 December 2002 and 28-29 February 2003. On 06-07 January 2003, the behaviour of OH temperature during the night shows a constant trend which is characterized by several short-period features. GWOs can be observed over a semidiurnal tidal feature on 29-30 March 2003. On 06-07 April 2003, GWOs can be observed over a linearly increasing trend. This was the general behaviour of nocturnal trend of OH temperature ~ short-period oscillations superimposed over a long period tidal feature. Herein, the short-period oscillations have been defined as the waves with periods of less than 3 h (following Fagundes *et al.*[7]).

In order to identify the short-period waves present in OH temperature series of a particular night, a filtering technique followed by Lomb-Scargle analysis was adopted. In the first step, the long term trend present during the night was identified wherever it was possible. As stated earlier, the tide-like oscillations were generally found to govern the long period variations of OH temperature. Hence, in order to identify the tidal features present, firstly, a sinusoidal least square fit of the form [$A\ Cos(2\pi t/T + \varphi) + c$] was forced on the OH time series with the wave period, T, as 8 h, 12 h and 24 h for a particular night, and then root mean square error was estimated for each value of T (here, A, is the amplitude of wave; T, the wave period; φ, represents the phase of the wave; and c, the constant term). The fit having the least value of the root mean square error was then assumed to be the tidal trend present in the data. Afterwards, the long-period tidal variation was removed from the raw data to bring out the short-period features, and the rest were defined as the residual dataset. This was followed by Lomb-Scargle analysis of the residual dataset to identify the harmonics. Lomb-Scargle periodogram analysis is a powerful tool to identify spectral components in an unevenly spaced sampling and test their significance[23]. Once the principal spectral components were identified (at alpha = 0.05), a waveform was reconstructed using the information of amplitude and phase of these spectral components and was applied to the residual dataset. Such analysis procedure has been commonly used to infer the wave periodicities in the MLT temperature measurements[24,25].

3.1 Case study of 07-08 November 2002

The observed variations of OH temperature on the night of 07-08 November 2002 is shown in top panel of Fig. 2. The sinusoidal least square fit analysis for

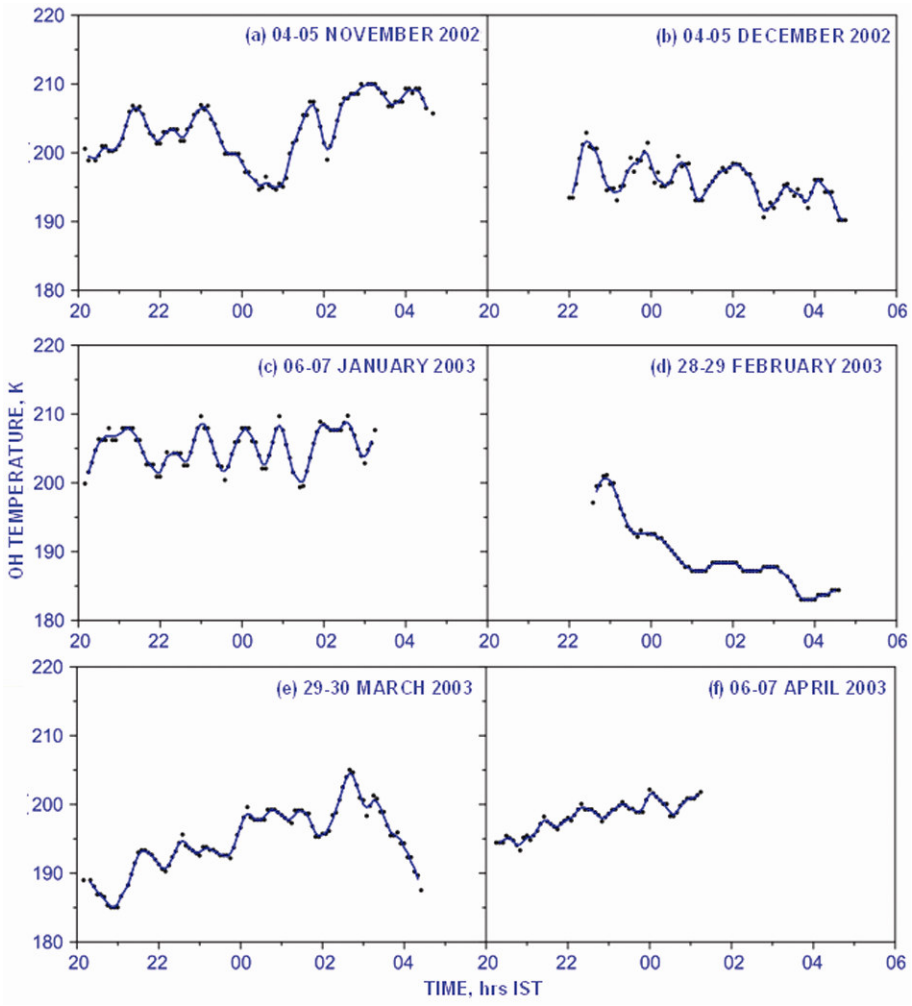

Fig. 1 — Typical examples of short-period oscillations (induced by gravity wave activity) observed in OH temperature

T = 8, 12 and 24 h suggests that the long-period variation of OH temperature on this night is governed by an 8 h tide, and this fact can be visualized from the plot of temperature in Fig. 2 itself. This 8 h wave [shown by the solid curve in Fig. 2(a)] had amplitude of ~6 K and phase of ~15.2 h. In the next step, the contribution of 8 h tide was removed from the raw data to get residual data. The bottom panel of Fig. 2 presents the plot of the residual data. Lomb-Scargle analysis of the residual data was performed to identify the gravity wave periods. It indicates the presence of 1.1, 1.4, 1.7 and 3.1 h waves with amplitude of 2.2, 2.4, 2.3 and 1.7 K, respectively. Table 1 summarizes the period, amplitude and phase of the different spectral components present in the residual data.

Based on this information, a waveform was reconstructed using superposition of these four waves and is shown by solid curve in Fig. 2 (b). A close correspondence between the peaks observed in the residual data and that of constructed waveform can clearly be seen. So far as the relative contribution of harmonics to the observed variability is concerned, the 1.1, 1.4 and 1.7 h waves shared the equivalent contribution, while the 3.1 h wave had somewhat smaller contribution (~ 18%).

3.2 Case study of 04-05 December 2002

The variation of temperature on this particular night is shown in Fig. 1 (b). A glance at temperature plot suggests that the nocturnal variation is diurnal in nature. However, the sinusoidal best fitting analysis suggests that the observed long period variation is due to a semidiurnal tide (having amplitude and phase of 2.3 K and 2.5 h, respectively). This semidiurnal component was removed from the original temperature data and Fig. 3 presents the variability of residual data during the night. Using Lomb-Scargle analysis, it was found that a mixture of 1.1 and 1.8 h wave explains the

variations of residual data with contribution of ~ 54 and 46%, respectively. Both the waves had amplitude of ~1.7 K. As done for 07-08 November 2002, a waveform using these two spectral components was constructed and is shown by solid curve in Fig. 3. Like noted earlier, a similarity in the observed variations and reconstructed waveform can be seen.

3.3 Case study of 06-07 January 2003

Figure 1(c) presents the behaviour of OH temperature on the night of 06-07 January 2003. As stated earlier, the gravity wave induced variations can be seen outlined over a constant trend. Unlike other nights, wherein the tidal trend was isolated from the original data, the temperature series of this particular night was de-trended to remove the linear trend present. Most probably, the gravity wave induced variations masked the semidiurnal or diurnal trend present in temperature series. The variation of residual temperature series is shown in Fig. 4. On this night, two waves having period of 1.7 and 2.5 h were present. Each wave had amplitude of ~2.1 K and equivalent contribution. The waveform that was reconstructed using these two harmonics is shown as the solid curve in Fig. 4.

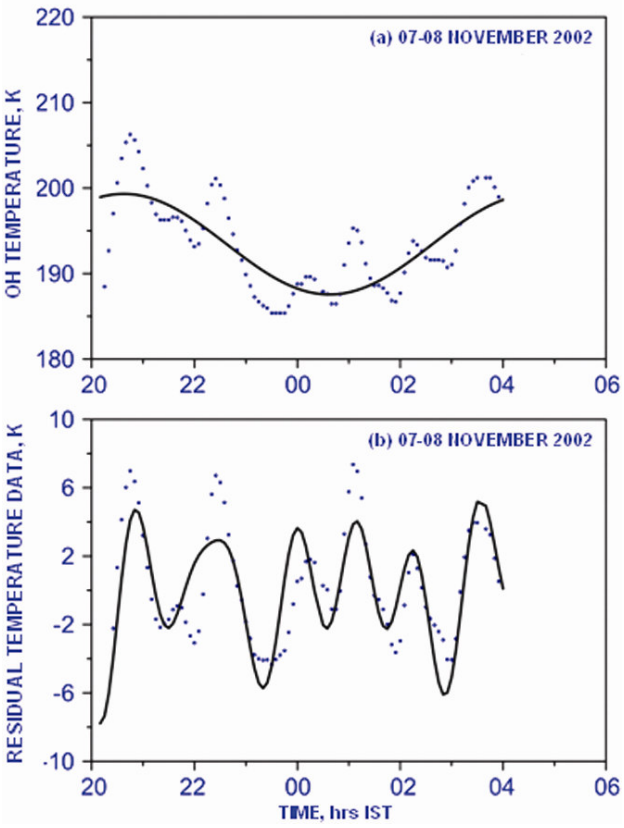

Fig. 2 — Nocturnal variation of OH temperature on 07-08 November 2002: (a) together with the sinusoidal least square fit of an 8 h tide (shown by solid curve); (b) variation of residual data (obtained by removing the 8 h tidal contribution from the raw data) along with the reconstructed waveform (shown by solid curves)

3.4 Case study of 28-29 February 2003

Figure 1(d) shows the behaviour of temperature on this particular night. Using sinusoidal best fit analysis, it was found that long period variation was driven by a diurnal tide. This diurnal tidal contribution was removed from original data and Lomb-Scargle analysis of residual data was performed. Figure 5

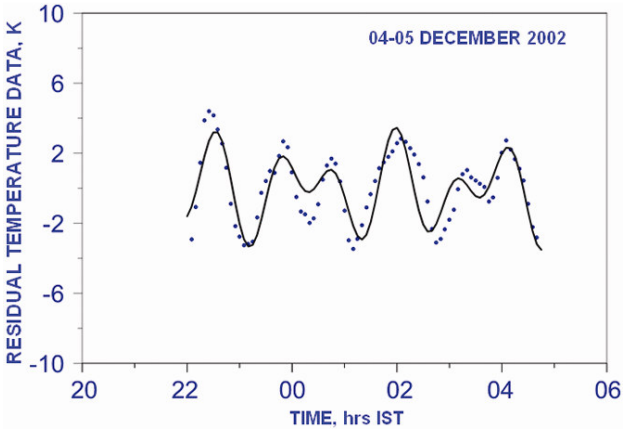

Fig. 3 — Nocturnal variability of the residual temperature (obtained by removing the 12 h tidal component from original temperature data) on 04-05 December 2002 along with the waveform reconstructed using 1.1 and 1.8 h wave

Table 1—Period, amplitude and phase of short-period waves deduced from Lomb-Scargle analysis

Day	1st Principal component			2nd Principal component			3rd Principal component			4th Principal component		
	Period (T), h	Amplitude (A), K	Phase (φ), h	Period (T), h	Amplitude (A), K	Phase (φ), h	Period (T), h	Amplitude (A), K	Phase (φ), h	Period (T), h	Amplitude (A), K	Phase (φ), h
07-08 Nov 2002	3.1	1.7	– 12	1.7	2.1	7.8	1.4	2.3	– 14	1.1	2.2	– 11
04-05 Dec 2002	1.8	1.7	12	1.1	1.8	15	-	-	-	-	-	-
06-07 Jan 2003	2.5	2.1	7	1.7	2.1	4	-	-	-	-	-	-
28-29 Feb 2003	4	1.6	7	1.4	1.2	– 3	-	-	-	-	-	-
29-30 Mar 2003	4.7	1.2	12	2.5	2.1	– 6	1.3	1.5	– 8	-	-	-

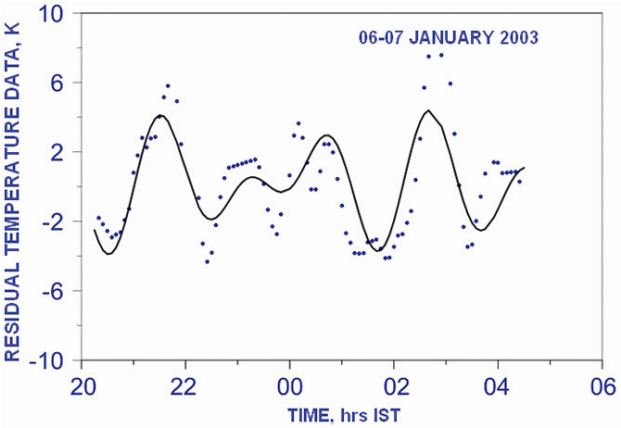

Fig. 4 — Nocturnal variability of the residual temperature (obtained by removing the 12 h tidal component from original temperature data) on 06-07 January 2003 along with the waveform reconstructed using 1.7 and 2.5 h wave

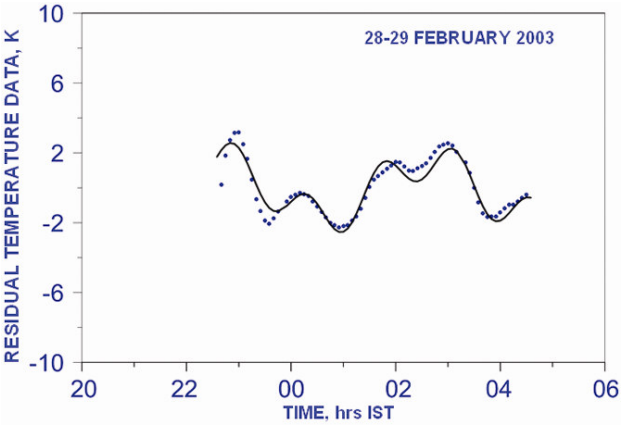

Fig. 5 — Nocturnal variability of the residual temperature (obtained by removing the 12 h tidal component from original temperature data) on 28-29 February 2003 along with the waveform reconstructed using 1.4 and 4 h wave

presents the behaviour of residual data during the night. Two waves having period of 1.4 and 4 h were identified to account for the observed variation. It was observed that the 4 h wave was the dominant component with a contribution of ~66%. The amplitude of 1.4 and 4 h wave was 1.2 and 1.6 K, respectively. A waveform was created using 1.4 and 4 h wave, and is shown by solid curve in Fig. 5. The dominance of 4 h wave in the observed variability can clearly be seen in Fig. 5. Of all the example of waveform fitting presented here, the best correspondence between residual temperature and applied waveform was observed on this particular night.

3.5 Case study of 29-30 March 2003

The behaviour of temperature on this particular night is shown in Fig. 1(e). A semidiurnal tide (having

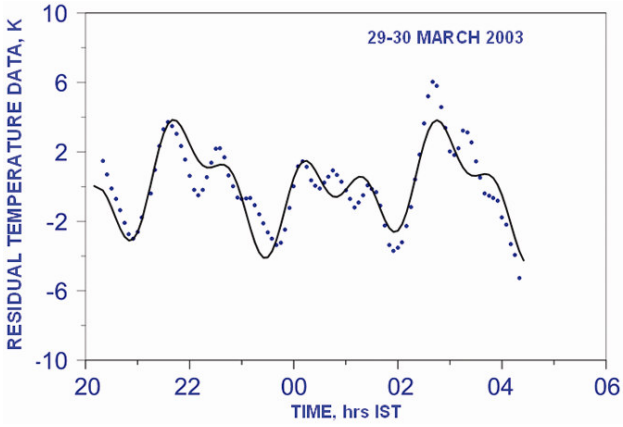

Fig. 6 — Nocturnal variability of the residual temperature (obtained by removing the 12 h tidal component from original temperature data) on 29-30 March 2003 along with the waveform reconstructed using 1.3, 2.5 and 4.7 h wave

amplitude and phase of ~6.1 K and ~0.6 h, respectively) was found to govern the temperature variation during the night. Lomb-Scargle analysis of residual temperature series indicates the presence of three waves with period of 1.3, 2.5 and 4.7 h. The 2.5 h wave strongly governed the observed variation of residual temperature with a contribution of 56%; while, the 1.3 and 4.7 h wave had equal contribution of 22%. The amplitude of the 1.3, 2.5 and 4.7 h wave was 1.5, 2.1 and 1.2 K, respectively. The observed variability of residual temperature and the waveform created using spectral components is shown in Fig. 6.

4 Conclusions

Gravity waves play a crucial role in the dynamics of the MLT region. While propagating upwards from the lower atmosphere, GWs encounter the background winds and undergo filtering action. A fraction of these upward propagating waves overcome wind filtering and reach the MLT heights where they dissipate momentum and energy. Often these waves are observed in airglow emissions from the MLT region as intensity variations. Nightglow measurements of OH (8, 3) Meinel band were made out at Kolhapur (16.8ºN, 74.1ºE), India during November 2002 – May 2003 using two tilting filter photometers. The OH rotational temperatures ~ a proxy of atmospheric temperature around the OH emission layer (at 87 km) were derived from the intensity information of $P_1(2)$ and $P_1(4)$ rotational line of OH (8, 3) Meinel band. The experiments were carried out with an objective to investigate the gravity wave activity in the temperature field of the MLT region over Kolhapur. On most of the nights, short-period oscillations

superimposed over long period tide-like variations were observed in OH temperature series. For the nights presented herein, the period of gravity wave induced oscillations lie in the range of 1.1 – 3.1 h. On few occasions, the 4 – 5 h waves were also observed. The periodicities observed herein correspond to those of the medium-scale gravity waves[27]. While the small-scale waves (having wavelength <100 km and time period <30 min) are more abundant but are more susceptible to wind-filtering. Medium-scale waves [having wavelength >100 km and time period of the order of a few tens of minutes (significantly greater than those of small-scale waves)] are generally capable of overcoming wind-filtering[27]. Most of the earlier reports from the Indian subcontinent using airglow measurements[12,14-16] have addressed the short-period gravity waves.

The amplitude of the observed gravity waves was found to vary between 1.2 and 2.4 K. The wave periodicities observed herein are larger than those reported by Taori *et al.*[16] using OH and O_2 temperature measurements and lidar observations. Taori *et al*. found 0.4 – 0.6 h waves to be prominent feature of the 40 – 95 km altitude range. Earlier, Parihar *et al.*[26] have reported observations of gravity waves in OH temperature and OI 557.7 nm emission during November 2003 to May 2005 wherein they observed the dominance of 2 – 3 h gravity waves. Taori & Taylor[24] reported the wave periodicities in the range of 0.8 – 12 h over Hawaii (20.8°N, 156.2°W). On few occasions, the authors found the amplitude of 2 h waves to be around 4 K (higher than those observed over Kolhapur). As the nightglow features were monitored along zenith only, the horizontal wavelengths and phase speed the observed gravity waves could not be inferred. Simultaneous measurements of OH Meinel band, O_2 Atmospheric band and OI 557.7 nm emission along with the wind information should have thrown more light into the vertical propagation characteristics of the observed gravity waves. In future, a comprehensive database of simultaneous measurements of different nightglow emissions from the MLT region along with MF radar wind measurements will be taken up to study the gravity wave field over Kolhapur.

Acknowledgement

Nightglow measurements have been carried out at Kolhapur, India under scientific collaboration between Indian Institute of Geomagnetism, Navi Mumbai and Shivaji University, Kolhapur. The funds for the research studies are being provided by Department of Science and Technology (DST), Govt of India, New Delhi. The grants received under CAWSES India Phase II programme from Indian Space Research Organization are gratefully acknowledged.

References

1 Fritts D C & Alexander M J, Gravity wave dynamics and effects in the middle atmosphere, *Rev Geophys (USA)*, 41 (1) (2003) 1003, doi: 10.1029/2001RG000106.

2 Hines C O, Internal atmospheric gravity waves at ionospheric heights, *Can J Phys (Canada)*, 38 (1960) pp 1441-1481.

3 Lindzen R S, Turbulence and stress owing to gravity wave and tidal breakdown, *J Geophys Res (USA)*, 86 (1981) pp 9707-9714.

4 Zhang Y, Xiong J, Liu L & Wan W, A global morphology of gravity wave activity in the stratosphere revealed by the 8-year SABER/TIMED data, *J Geophys Res (USA)*, 117 (2012) D21101, doi: 10.1029/2012JD017676.

5 Cowling D H, Webb H D & Yeh K C, Group rays of internal gravity waves in a wind-stratified atmosphere, *J Geophys Res (USA)*, 76 (1971) pp 200–213.

6 Medeiros A F, Takahashi H, Buriti R A, Pinheiro K M & Gobbi D, Atmospheric gravity wave propagation direction observed by airglow imaging in the South American sector, *J Atmos Sol-Terr Phys (UK)*, 67 (2005) pp 1767-1773.

7 Fagundes P R, Takahashi H, Sahai Y & Gobbi D, Observations of gravity waves from multispectral mesospheric nightglow emissions observed at 23°S, *J Atmos Terr Phys (UK)*, 57 (4) (1995) pp 395-405.

8 Bageston J V, Wrasse C M, Gobbi D, Takahashi H & Souza P B, Observation of mesospheric gravity waves at Comandante Ferraz Antarctica Station (62° S), *Ann Geophys (Germany)*, 27 (6) (2009) pp 2593-2598.

9 Li Z, Liu Alan Z, Lu Xian, Swenson Gary R & Franke Steven J, Gravity wave characteristics from OH airglow imager over Maui, *J Geophys Res (USA)*, 116 (2011) D22115 pp 1-22.

10 Goldberg R A, Fritts D C, Schmidlin F J, Williams B P, Croskey C L, Mitchell J D, Friedrich M, Russell J M III, Bium U & Fricke K H, The MaCWAVE program to study gravity wave influences on the polar mesosphere, *Ann Geophys (Germany)*, 24 (4) (2006) pp 1159-1173.

11 Nielsen K, Taylor M J, Pautet P –D, Fritts D C, Mitchell N, Beldon C, Williams B P, Singer W, Schmidlin F J & Goldberg R A, Propagation of short-period gravity waves at high-latitudes during the MaCWAVE winter campaign, *Ann Geophys (Germany)*, 24 (4) (2006) pp1227-1243.

12 Mukherjee G K, The signature of short-period gravity waves imaged in the OI 557.7 nm and near infrared OH nightglow emission over Panhala, *J Atmos Sol-Terr Phys (UK)*, 65 (2003) pp 1329-1335.

13 Dutta G, Tsuda Toshitaka, Kumar P Vinay, Kumar M C Ajay, Alexander Simon P & Kozu Toshiaki, Seasonal variation of short-period (<2 h) gravity wave activity over Gadanki, India (13.5°N, 79.2°E), *J Geophys Res (USA)*, 113 (2008) D14103, pp 1-13.

14 Mukherjee G K, Sikha Pragati R, Parihar N, Ghodpage Rupesh & Patil P T, Studies of the wind filtering effect of gravity waves observed at Allahabad (25.45° N, 81.85° E) in India, *Earth Planet Space (Japan)*, 62 (3) (2010) pp 309-318.

15 Lakshmi Narayanan V & Gurubaran S, Statistical characteristics of high frequency gravity waves observed by OH airglow imaging from Tirunelveli (8.7°N), *J Atmos Sol-Terr Phys (UK)*, 92 (2013) pp 43-50.

16 Taori A, Kamalakar V, Raghunath K, Rao S V B & Russell J M III, Simultaneous Rayleigh lidar and airglow measurements of middle atmospheric waves over low latitudes in India, *J Atmos Sol-Terr Phys (UK)*, 78-79 (2012) pp 62-69.

17 Mukherjee G K & Parihar N, Measurement of rotational temperature at Kolhapur, India, *Ann Geophys (Germany)*, 22 (2004) pp 3315-3321.

18 Mukherjee G K & Dyson P L, A filter tilting photometer for nightglow measurements of 630.0 nm emission line, *Indian J Radio Space Phys*, 92 (1992) pp 212.

19 Mies F H, Calculated vibrational transition probabilities of OH($X^2\prod$), *J Mol Spectrosc (USA)*, 53 (2) (1974) pp 150-188.

20 Parihar N & Mukherjee G K, Measurement of mesopause temperature from Hydroxyl nightglow at Kolhapur (16.8°N, 74.2°E), India, *Adv Space Res (UK)*, 41 (4) (2008) pp 660-669.

21 Kendall D J W & Clark T A, The pure rotational atmospheric lines of hydroxyl, *J Quant Spectrosc Radiat Transf (UK)*, 21 (1979) pp 511-518.

22 Langhoff S R, Werner H J & Rosmus P, Theoretical transition probabilities for the OH Meinel system, *J Mol Spectrosc (USA)*, 118 (1986) pp 507-529.

23 Lomb N R, Least-squares frequency analysis of unequally spaced data, *Astrophys Space Sci (Netherlands)*, 39 (1976) pp 447-462.

24 Taori A & Taylor M, Characteristics of wave induced oscillations in mesospheric O_2 emission intensity and temperatures, *Geophys Res Lett (USA)*, 33 (2006) L01813, doi: 10.1029/2005GL024442.

25 Taori A & Parihar N, Simultaneous bi-station measurements of mesospheric waves from Indian low latitudes, *Adv Space Res (UK)*, 48 (2011) pp 218-226.

26 Parihar N, Gurubaran S & Mukherjee G K, Observations of OI 557.7 nm nightglow at Kolhapur (17°N), India, *Ann Geophys (Germany)*, 29 (2011) pp1873-1884.

27 Vadas S L, Taylor M J, Pautet P –D, Stamus P A, Fritts D C, Liu H –L, Sabbas F T Sao, Rampinelli V T, Batista P & Takahashi H, Convection: the likely source of medium-scale gravity waves observed in the OH airglow layer near Brasilia, Brazil, during the SpreadFEx campaign, *Ann Geophys (Germany)*, 27 (2009) pp 231-259.